Studies of Spherical Tori, Stellarators and Anisotropic Pressure with M3D[1]

L.E. Sugiyama 1), W. Park 2), H.R. Strauss 3), S.R. Hudson 2), D. Stutman 4), X-Z. Tang 2)

1) Massachusetts Institute of Technology, Cambridge MA, U.S.A
2) Princeton Plasma Physics Laboratory, Princeton NJ, U.S.A
3) New York University, New York, NY, U.S.A
4) Johns Hopkins University, Baltimore MD, U.S.A.

e-mail contact of main author: sugiyama@psfc.mit.edu

Abstract. The M3D (Multi-level 3D) project simulates plasmas using multiple levels of physics, geometry, and grid models in one code package. The M3D code has been extended to fundamentally nonaxisymmetric and small aspect ratio, $R/a \gtrsim 1$, configurations. Applications include the nonlinear stability of the NSTX spherical torus and the spherical pinch, and the relaxation of stellarator equilibria. The fluid-level physics model has been extended to evolve the anisotropic pressures $p_{j\|}$ and $p_{j\perp}$ for the ion and electron species. Results show that when the density evolves, other terms in addition to the neoclassical collisional parallel viscous force, such as $\mathbf{B}\cdot\nabla p_e$ in the Ohm's law, can be strongly destabilizing for nonlinear magnetic islands.

1. Introduction

The M3D (Multi-level 3D) project [1] simulates plasmas using multiple levels of physics, geometry, and grid models in one code package. The M3D code has been extended to fundamentally non-axisymmetric and small aspect ratio, $R/a \gtrsim 1$, configurations. Applications include the NSTX spherical torus, the spherical pinch, and stellarators. The fluid-level physics model has been extended to evolve the anisotropic pressures $p_{j\|}$ and $p_{j\perp}$ for the ions and electrons, which includes the neoclassical, collisional parallel viscous stresses.

2. The Spherical Torus

NSTX discharges experience internal reconnection events (IRE), with substantial global energy loss, when the value of the safety factor q in the core is near 2 or 1. Cases with $R/a = 1.3$ and peak beta about 10% were studied using M3D. When the core $q \simeq 2$, both experimental data and simulation indicate that a double tearing reconnection associated with the existence of two $q = 2$ surfaces causes an IRE. Experimental soft X-ray (SXR) data shows the core crash propagates inward from off-axis. Simulation suggests that a single $q = 2$ surface tends to be stable. Figure 1a shows simulated temperature contours during a double tearing reconnection, where the growing inner $m = 2$ islands encroach on the core region. Figure 1b shows the calculated SXR signals in time and Fig. 1c the temperature contours from the calculated ECE signals, in the (r, t) plane. At present, it is difficult to compare SXR signals between experiment and theory because the experiment (so far) is ohmic and the plasma rotates slowly and, in addition, the theoretical signals show no strong distinguishing features (compare the $q \simeq 1$ case, below). The T_e contour plot (Fig. 1c), on the other hand, maps the topological changes clearly. One can see, e.g., the core region being completely reconnected with the inner $m = 2$ islands. Although ECE detection is not feasible in NSTX, the planned EBW (Electron Bernstein Wave) measurement of temperature should allow a detailed comparison with theory.

[1]This work was supported in part by the U.S. Department of Energy.

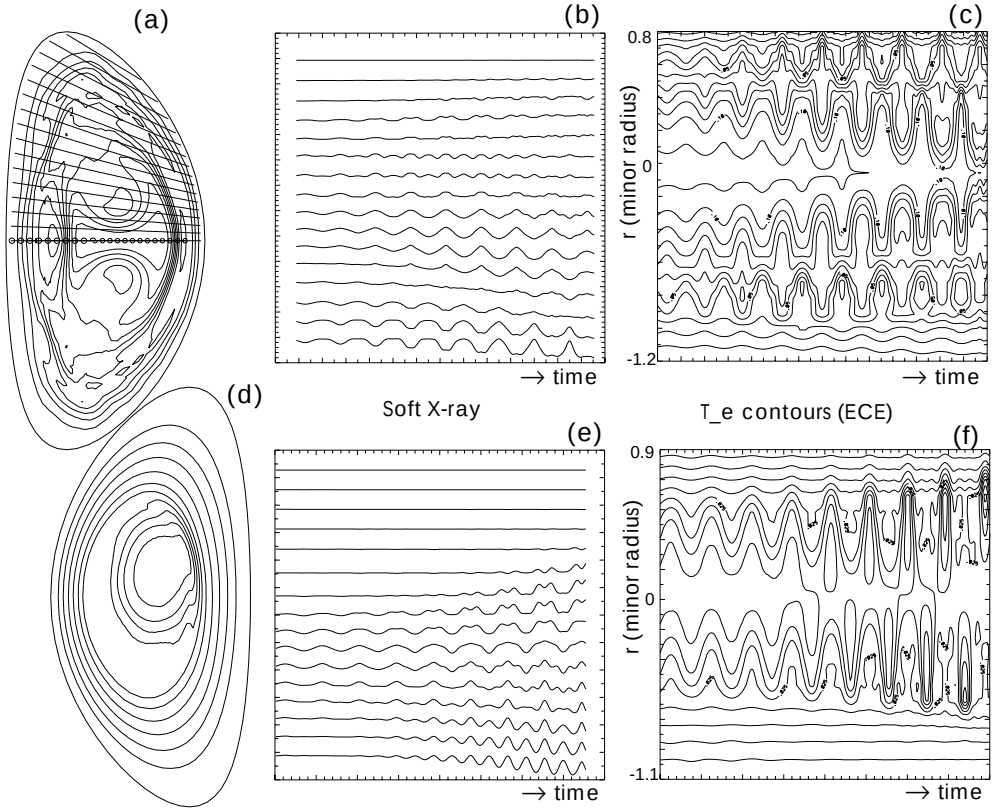

FIG. 1. Simulation results for two types of IREs in NSTX. Double tearing reconnection with core $q \simeq 2$, a) temperature contours, also showing lines of sight for the simulated SXR and midplane positions for the ECE signals, b) time plot of SXR signals, c) ECE signals, shown as T_e contours on the (r,t) plane. Case with core $q \simeq 1$, d) temperature contours, e) SXR, and f) ECE.

A case with $q \simeq 1$ is shown in Figs. 1d–f. The SXR signals show a classic sawtooth precursor, as does experiment (not shown). Experimental data further shows that the plasma rotation slows before the final crash, possibly locking to the resistive wall. There are also indications that a localized medium-n (toroidal mode number) instability develops just before the final crash. This could be driven by the local pressure bulge produced by the initial low-n modes, as in high-β tokamak disruptions [2]. These questions are being further investigated.

3. The Spherical Pinch

The Spherical Pinch (SP) is a promising low aspect ratio toroidal device with a reversed shear rotational transform, which combines features of the spherical torus and the pinch. Toroidal pinches have poloidal and toroidal components of the magnetic field of comparable magnitude, $qR/a \sim 1$. They tend to have reversed magnetic shear, which can be favorable for confinement. Reversed field pinches typically have $R/a \sim 5$, $q \sim 0.2$. Confinement is poor due to MHD activity, because of the many resonances with poloidal mode number $m = 1$. SP's have $R/a \sim 1$, $q \sim 1$ and can be made with $1 > q > \hat{m}/(\hat{m}+1)$. Taking $\hat{m} \geq 1$ eliminates the $m = 1$ resonances. These special SP's have a monotonically decreasing q-profile. The toroidal field is small at the outer edge, but does not reverse; unlike a spheromak, there is an applied toroidal magnetic field.

Ideal MHD simulations were done with a poloidal unstructured mesh [3][4] of 2500 points and spectral representation in toroidal angle. The plasma had $R/a = 1.5$ and a rigid, conducting wall boundary. Typical equilibrium profiles are shown in Fig. 2a,b.

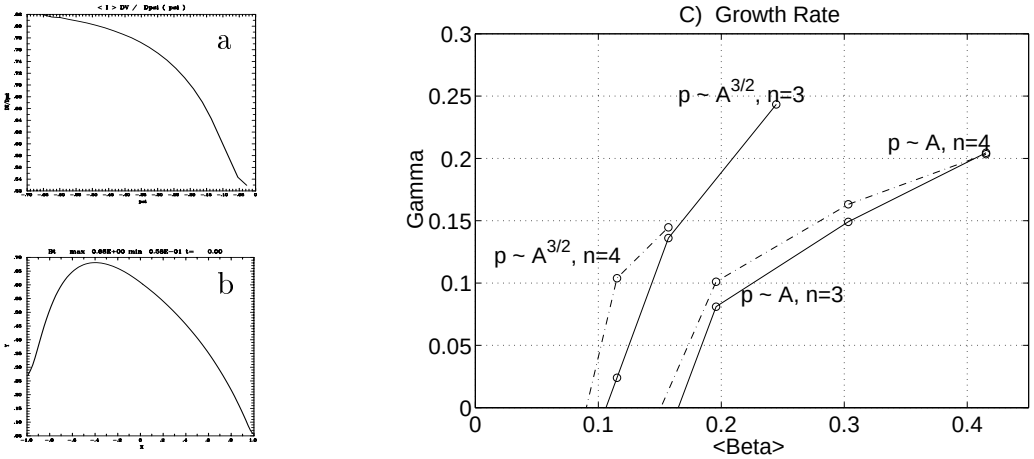

FIG. 2. SP equilibrium profiles of a) q and b) toroidal magnetic field B_T as functions of R, $p \sim \psi$, and $\langle\beta\rangle = 12\%$. c) Growth rate versus $\langle\beta\rangle$ for $n = 3, 4$ modes, for equilibria with $p \sim \psi$ and $\psi^{3/2}$.

SP's are MHD stable below a $\langle\beta\rangle$ threshold ($\langle\beta\rangle \equiv 2\langle p\rangle/\langle B^2\rangle$, where the bracket is an average over the poloidal plane). Stability is determined by "reverse ballooning" modes, which resemble low-mode-number ballooning modes, but have maximum amplitude on the inboard, high field side, apparently due to the reversed shear and low aspect ratio. In the example, modes with $(m, n) = (2, 3)$ and $(3, 4)$ are unstable (Figs. 2c and 3a). The critical $\langle\beta\rangle$ depends on the shape of the equilibrium pressure profile. Fig. 2c compares two profiles, $p \sim \psi$ and $p \sim \psi^{3/2}$, at toroidal mode numbers $n = 3$ and 4. The broader profile, $p \sim \psi$, is more stable, with critical $\langle\beta\rangle \simeq 15\%$. Yet broader profiles may have higher $\langle\beta\rangle$. (The marginal points were interpolated from stable, damped modes.)

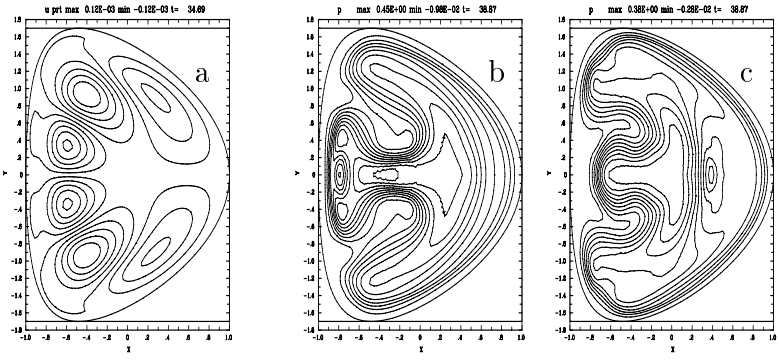

FIG. 3. a) Velocity potential of the (3,4) linear mode in the poloidal plane $\phi = 0$, for the equilibrium of Fig. 2a,b. Nonlinear "reverse ballooning" pressure contours at $t = 37\tau_A$, at b) $\phi = 0$ and c) $\phi = \pi$.

Nonlinearly, an unstable high-β SP with reversed shear disrupts by distortion of the high field side. The lowest mode numbers appear to dominate the evolution (Fig. 3b,c).

4. Stellarators

To model stellarators, M3D uses a mesh with a three dimensional spatial variation. Output from the VMEC code [5] can be used to construct an initial M3D equilibrium. This initial state is then relaxed under the influence of resistive dissipation, cross field thermal conduction, and parallel thermal conduction (simulated with the "artificial sound" method), using source terms to maintain the toroidal current and pressure. The kinetic energy is removed by viscous damping. Equilibria have been obtained for LHD, W7-AS, and the proposed NCSX compact quasi-axisymmetric (QAS) stellarator. Detailed comparison with the PIES code [6] is in progress.

The QAS simulations used a mesh of 6000 poloidal points $\times$ 36 toroidal planes. Figure 4

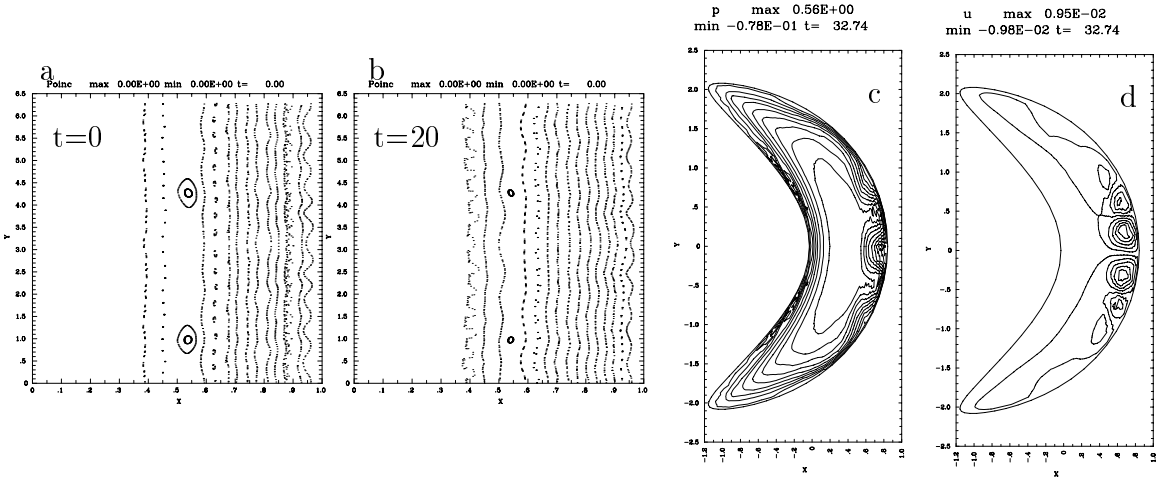

FIG. 4. QAS stellarator. a,b) Field line plots showing the relaxation of equilibrium li383 from a) an initial VMEC equilibrium at $t = 0$ to b) $t = 20\tau_A$. At twice the pressure, the configuration is ballooning unstable, as shown by the contours of c) pressure and d) velocity potential at $t = 32\tau_A$.

shows the relaxation of QAS equilibrium li383 at the design pressure. Although VMEC assumes perfect flux surfaces, its output current lacks the singularities needed to prevent island formation at rational surfaces. When this current is used to calculate the initial magnetic field in M3D, the configuration contains islands (Fig. 4a). The islands tend to shrink during relaxation (Fig. 4b). At high enough pressure, however, the plasma becomes unstable to ballooning modes (Fig. 4c,d).

5. Anisotropic fluid pressure

To improve the fluid (MHD/two-fluid/neoclassical) description of a confined plasma, the anisotropic pressure components $p_{||}$ and $p_\perp$ can be evolved and the moments closed using the heat fluxes $q_{||}$ and $q_\perp$. M3D now evolves the anisotropic temperatures $T_{j||}$ and $T_{j\perp}$ for electrons and ions j, through equations for the average temperatures $T_j = (T_{j||} + 2T_{j\perp})/3$ and the anisotropies $\delta T_j = T_{j||} - T_{j\perp}$, using a collisional form of the δT equations with relatively simple expressions for the collision terms. The density (continuity) equation is solved separately. The M3D heat fluxes include the effects of parallel and cross field thermal conduction, the parallel part modelled as thermal equilibration along magnetic field lines ("artificial sound").

The collisional parallel viscous forces $\nabla \cdot \mathbf{\Pi}_{||}$, $\mathbf{\Pi}_{||} = \delta p(-\mathbf{I}/3 + \hat{\mathbf{b}}\hat{\mathbf{b}})$ where $\delta p = n\delta T$, appear naturally, including the neoclassical enhancement to the polarization drift. Studies with M3D have shown [7] that in a torus the dominant role is played by the flux surface average of the viscous forces, rather than by (simple forms of) the poloidal variation, for the bootstrap current and other effects on the equilibrium and on the neoclassical tearing mode (NTM).

The neoclassical pressure anisotropy in $\nabla \cdot \mathbf{\Pi}_{||}$ becomes significant only at relative high β and low resistivity. For the (2,1) resistive NTM, M3D results show that the related, two-fluid term $(1/en)\nabla_{||} p_e$ in the Ohm's law may also nonlinearly destabilize magnetic islands, at lower β. It has no effect on the linear mode. Although typically $\mathbf{B} \cdot \nabla T_e \simeq 0$, $\mathbf{B} \cdot \nabla p_e$ is not if the density is allowed to evolve. In equilibrium, $(\nabla_{||} n)/n \sim O(\delta p/p)$. Nonlinearly, the density equilibrates along field lines, due to the effects of sound waves acting on the pressures and perpendicular thermal conduction, which are slow compared to the electron temperature equilibration. This was confirmed by applying an accelerated parallel equilibration to p_e at fixed density, rather than to T_e, when the entire gradient ∇p_e was kept in the Ohms' law. The island then behaved

like the ordinary resistive MHD case without ∇p_e. Adding the rest of the two-fluid terms did not greatly change the nonlinear rate of growth compared to just $\nabla_{||} p_e$.

Simulations show that the nonlinear growth/shrinkage of magnetic islands and its correlation with terms in the parallel Ohm's law is not simple. In NTM theory, the pressure gradient flattens over a finite-size island and the additional, flux surface averaged bootstrap current $\propto \langle dp/d\psi \rangle$ drives island growth. The collisional viscous stress term calculated from evolving δT is more variable and its flux surface average (with respect to the equilibrium field) tends to overshoot to positive values inside a growing island, rather than tending to zero (Fig. 5).

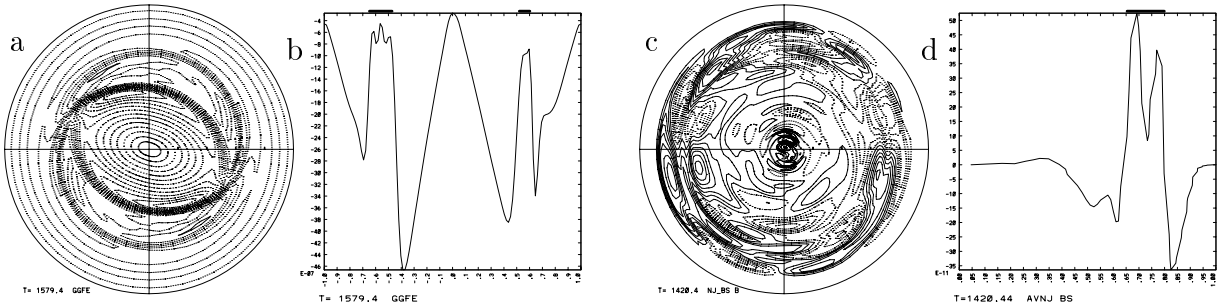

FIG. 5. Parallel component of the electron collisional parallel viscous force $X_e = (1/(enB^2))\mathbf{B} \cdot \nabla \cdot \mathbf{\Pi}_{e||}$ for large (2,1) islands. First case (a,b) uses the neoclassical expressions for ions and electrons, shows $X_e \simeq (1/3enB)(nm_j/\tau_j)\mu_{0j}U_{\theta j}$ where μ_{0j} is the neoclassical coefficient for the flow $U_{\theta j}$, with equilibrium $\nabla T_j = 0$ [7]. a) Contours and b) profile as a function of minor radius, left side along $\theta = \pi/2$ in (a) (upper vertical axis) and right side along $\theta = 0$ (right horizontal axis). Second case (c,d) evolves δT_j with $\nabla T_j \neq 0$. c) Contours and d) flux surface average, based on the equilibrium field, as function of minor radius [0,a]. Axis and edge values are zero. Top bars show location of islands.

The nonlinear terms — two-fluid, parallel gradient, and δT_j — can also introduce significant $(2m, 2n)$ components (e.g., Fig. 5c). Certain terms, including the Ohm's law $\nabla_{||} p_e$ and $\nabla \cdot \mathbf{\Pi}_{e||}$, also drive island rotation. Resistive MHD islands tend to remain (2,1), but the other effects, especially two-fluid, can lead to development of a (4,2) structure inside the original outer (2,1) structure. The (4,2) magnetic field lines are disjoint, i.e., each pair of opposite O-points shares field lines within, but not between, pairs. Other effects also exist, since small resistivity alone is found to be nonlinearly destabilizing in MHD and two-fluids, for islands that are stable or very slowly growing at higher resistivity.

References

[1] PARK, W., et al., "Plasma simulation studies using multilevel physics models," Phys. Plasmas **6** 1796 (1999).

[2] PARK, W. et al., "High-β disruption in tokamaks," Phys. Rev. Lett. **75** (1995) 1763.

[3] STRAUSS, H.R., LONGCOPE, D.W., "An adaptive finite element method for magneto-hydrodynamics," J. Comput. Phys. **147** (1998) 318.

[4] STRAUSS, H.R., PARK, W., "MHD effects on pellet injection in tokamaks," Phys. Plasmas **5** (1998) 2676.

[5] HIRSHMAN, S.P., WHITSON, J.C., "Steepest-descent moment method for three-dimensional magnetohydrodynamic equilibria," Phys. Fluids **26** 3553 (1983).

[6] RIEMAN, A.H., GREENSIDE, H.S., "Computation of zero β three-dimensional equilibria with magnetic fields," J. Comput. Phys. **87** (1990) 349.

[7] SUGIYAMA, L.E., and PARK, W., "A nonlinear two-fluid model for toroidal plasmas," Phys. Plasmas, to appear (2000).